JOURNAL OF CHEMICAL INFORMATION AND MODELING

Article

pubs.acs.org/jcim

Models for Predicting IKKA and IKKB Blockade

Haipeng Hu* and James P. Snyder*

Department of Chemistry, Emory University, Atlanta Georgia 30322, United States

Supporting Information

ABSTRACT: We describe the application of different methods in the development of QSAR models for IKKA and IKKB inhibition. The results show that the best QSAR models provide highly accurate predictions for existing IkB-kinase (IKK) inhibitors. The exceptions, corresponding to 5% of the known collection of inhibitors, are five classes of compounds incorporating the nitrile or sulfonamide moieties, small compounds with molecular weights of less than 300, and two classes of blockers considered to be type II kinase inhibitors. Comparison of our novel IKKB homology model and the recently reported IKKB crystal structure implies that a predictive protein−antagonist complex structure is more likely to exist as an inactive form in the crystalline state as observed in the recent protein X-ray structure.

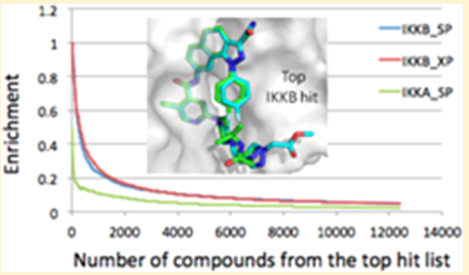

INTRODUCTION

The NF-kB family of nuclear transcription factors, composed of ubiquitously expressed proteins that regulate the transcription of numerous genes, are implicated in the induction of inflammatory disorders, cancers and diabetes, among others. The transcription factors reside in the cytoplasm of unstimulated cells and form inactive complexes with a family of inhibitor proteins known as IkBs. Until triggered, they mask the nuclear localization signals of NF-kB. The conversion of NF-kB to its active nuclear form, composed of p50 and p65 (Rel-A) subunits, is kindled by lipopolysaccharide (LPS) or cytokines. In response to various stimuli, IkB is phosphorylated by IkB-kinase (IKK) leading to its ubiquitination, proteosomal degradation, translocation of the active subunits to the nucleus, and activation of gene transcription.[1] IKK is a high molecular weight trimeric complex consisting of IKKA, IKKB, and NEMO. Although both IKKA and IKKB units are capable of phosphorylating IkBa, IKKB has been identified as essential for the activation of the complex in response to inflammatory stimuli. The potential for utilizing IKKB inhibitors in the treatment of cancer and immunological disorders has been widely recognized by the pharmaceutical industry.[2,3]

Because of the key role played by the inhibition of IKK in both the canonical and noncanonical activation pathways of NF-kB, the discovery and development of small molecule IKKB modulators has evolved into a significant area of study. In the past decade, many drug candidates that target IKK with preclinical efficacy have been reported. These include BMS-345541 and the Bayer "Compound A", which are effective in preclinical models of arthritis and the blockade of chronic pulmonary inflammation, respectfully.[4,5] Most of the reported IKK inhibitors have been catalogued in the online Binding Database (BindingDB).[6]

The present work describes the development of IKK homology models and discusses attempts to develop accompanying 3D-QSAR models for predicting blockade of the IKKA and IKKB kinases by employing training and test sets for IKK inhibitors with explicit IC_{50}values found in the BindingDB. We propose that the best QSAR models can be productively utilized for virtual screening of large compound libraries and the discovery of novel IKK inhibitor candidates.

RESULTS AND DISCUSSION

In this study, our major aim is to generate effective QSAR models for two subunits of IKK proteins as tools for IKK inhibitor discovery.

Homology Modeling and Crystal Structure of IKKs. Homology models of the IKKB and IKKA DLG-in and IKKB DLG-out conformations have been constructed with Modeller9v1[7] and Prime 3.1.[8] Comparison of the crystal structure of IKKB with our IKKB DLG-in homology model illustrates high structural similarity around the ATP binding pocket except for two regions: the G-rich loop region (red loops in Figure 1), and the activation segment linking the DLG motif and the conserved Ala-Phe-Glu (APE) motif (yellow loops in Figure 1, residues 166−192). In the crystal structure, since the IKKB inhibitor only occupies the adenosine region leaving the catalytic center empty, the G-rich loop has the opportunity to fold into the DLG motif. This closed conformation shrinks the volume of the catalytic center significantly. In the IKKB homology model, due to occupation of the catalytic center by AMP-PNP, the G-rich loop presents an open conformation. The activation segment, the other significantly different region between IKKB conformers, presents a pose covering the kinase substrate binding pocket in the crystal structure, which differs not only from the IKKB homology model but also from other activated protein kinases such as PKA (PDB ID 1ATP).

Due to the high sequence similarity between IKKA and IKKB (58% identity), the 3D structure of the IKKA homology

Received: June 20, 2012
Published: November 19, 2012

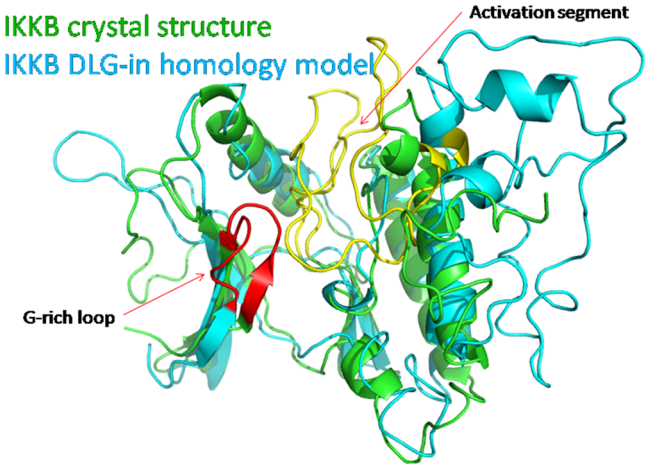

Figure 1. Superposition of the IKKB crystal structure (PDB ID 3RZF) and the IKKB DLG-in homology model. The G-rich loop is shown in red, and the activation segment is shown in yellow.

model is essentially superimposable with the IKKB crystal structure (backbone RMSD < 0.58 Å) as shown in Figure 2.

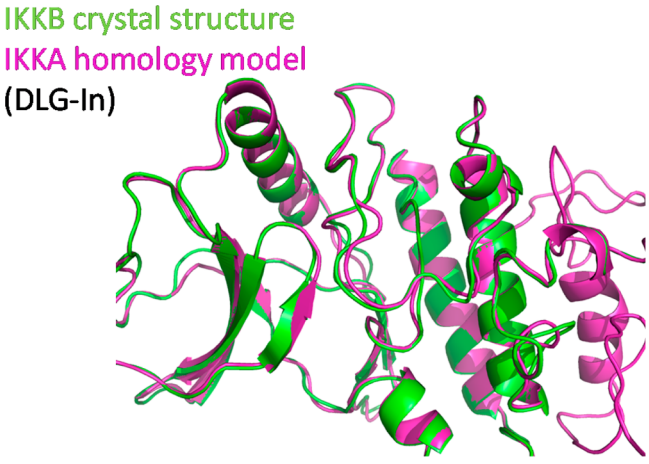

Figure 2. Superposition of the IKKB crystal structure (PDB ID 3RZF) and the IKKA homology model.

The IKKB DLG-out homology model shares high structural similarity with its template 1WBN but differs from the IKKB crystal structure in the G-rich loop and the activation segment induced by the conformational change of the DLG motif (see Figure 3).

Docking Studies. The Glide[9] and Prime applications in the Schrodinger Suite 2011 were investigated in an attempt to determine the most suitable scoring protocol for docking. Three different scoring functions (Glide SP, Glide XP, and MM/GBSA) were examined for all IKKA and IKKB blockers extracted from the BindingDB. Unfortunately, none proved to be consistent with the experimental pIC50 values (pIC50 = −log IC_{50}) for either enzyme. The corresponding correlation coefficients (R^2) linking docking scores and pIC50 quantities were uniformly <0.01. Thus, no meaningful linear correlation between the generally superior Glide-MM/GBSA scores and pIC50 values was achieved. We turned to another approach.

Neural Network Analysis.[10] As a consequence of the poor correlations described above, new scoring functions for the IKKA and IKKB homology models and the IKKB crystal

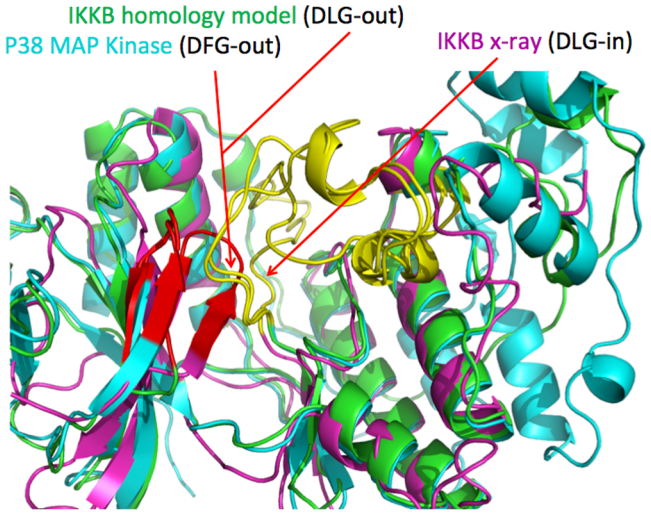

Figure 3. Superposition of the IKKB crystal structure, the P38 DFG-out conformation and the IKKB DLG-out homology model. The G-rich loops are shown in red and the activation segments are shown in yellow. Locations of DLG loops indicated by red arrows.

structure were constructed. Although Glide SP, Glide XP, and MM/GBSA scores show no meaningful correlations with pIC50, the energy terms used in the scoring functions (VDW and polar interactions at the binding site, Coulombic energies, lipophilicity, H-bonding, metal-binding, penalties for buried polar groups and frozen rotatable bonds, etc.) are, nonetheless, valuable descriptors useful for generating alternative scoring functions with better predictability.

The descriptors utilized by Glide SP, Glide XP, and MM/GBSA were iteratively reweighted in Canvas1.5[11] to establish new scoring functions in the neural network framework. For each of the IKKA and IKKB inhibitor data sets, 70% were randomly selected as the training sets, while the remaining 30% were assigned to the test set. The predicted pIC50 values were compared with experimental pIC50s obtained from the literature. The model with the highest Pearson correlation coefficient (Pearson r) is considered to be the best fit. For IKKB, the best models from both the crystal structure and the homology model were obtained with Glide SP descriptors, and both provided the same Pearson r value (0.59). For IKKA, Glide XP descriptors provide the best statistical result (Pearson r = 0. 34), considerably worse than the IKKB model. All data are shown in Table 1. Thus, neural network analysis for the IKK data sets indicates that the best Pearson r for predicted IC_{50} quantities falls below 0.60 for which the ideal value is 1.

Field-Based QSAR. The field-based QSAR method (FB-QSAR)[12] is an implementation of the CoMFA/CoMSIA scheme with a specific set of parameters provided by the 2011 Schrodinger suite. The 3D-QSAR model is generated by

Table 1. Pearson Correlation Coefficients Relating Predicted pIC50 and Experimental pIC50 Values Derived from Neural Network Analysis

Pearson r	Glide SP	Glide XP	MM/GBSA
IKKA model	0.26	0.34	0.29
IKKB crystal	0.59	0.59	0.42
IKKB model	0.59	0.56	[a]

[a]Failed to converge.

dx.doi.org/10.1021/ci300287t | J. Chem. Inf. Model. 2012, 52, 3190−3199

partial least-squares (PLS) regression combined with either an electrostatic/steric force field or a Gaussian force field. The latter includes steric, electrostatic, hydrophobic, H-bond acceptor, and H-bond donor components expressed by the Gaussian formalism.[13] An improved R^2 for the training set can always be achieved with a larger number of PLS principal components (i.e., factor number). Frequently, however, the corresponding Pearson r can decrease unexpectedly accompanied by poor test set predictability. This situation signals an over fitted model.[14] In order to avoid this, a QSAR with a training set $R^2 \sim 0.8$ and a suitable Pearson r is favored as a superior model.

Prior to performing FB-QSAR analysis, the database compounds were generated as 3D structures and aligned with each other. A Schrodinger Suite utility, Flex-align, has been recommended for aligning sets of small compounds without target protein information. Alternatively, a docking study can provide compound alignment when the target protein structure is available. In the present study, both Flex-align and Glide SP and Glide XP docking were utilized as alignment methods.

Flex-align Alignment. The IKKA and IKKB inhibitor subsets were separately aligned by Flex-align. As in the neural network analysis, training and test sets were constructed with 70% and 30% of data set members, respectively.

The IKKB data set delivers a model with an R^2 of 0.85 and a Pearson r of 0.75, while IKKA provides an R^2 of 0.83. The somewhat less favorable Pearson r of 0.56 for IKKA indicates this model to be less predictive than that for IKKB. Since the inhibitor data sets were obtained from 28 references (2002–2011[15−42]) listed in the BindingDB and the compounds from the same report always share high structural similarity, we considered the possibility that the FB-QSAR models are biased by the excessively focused structural frameworks. Thus, the two data sets were ordered by Canvas's hierarchical clustering methodology. The 819 IKKB inhibitors were separated into 46 clusters, while the 384 IKKA inhibitors were clustered into 25 subsets. Clusters with more than 25 members were investigated further. For IKKB, all members of these clusters were selected to generate a new QSAR model. The latter provides similar statistical results by comparison with the full compound list (R^2 of 0.85 and Pearson r of 0.75; see Table 2). Given the lack of improvement by clustering, the full data set model was utilized in the following analysis. The IC_{50} values of the selected cluster compounds were predicted by this model as shown in Table 3. The largest cluster in IKKB, cluster 16 with a polycyclic scaffold (Figure 4**a**), provided the best statistical result. The remaining large clusters exhibit Pearson r values greater than 0.69 with the exception of cluster 38 (Table 3). Compounds in the latter present a linear unbranched scaffold, while cluster 37 furnishes a similar linear scaffold accompanied by a piperidine-derived sulfonyl-amide headgroup (Figure 4**b** and **c**). The average molecular weight of the compounds in these two clusters is about 30 Da higher than the average of the whole IKKB data set. This observation reveals that the flex-align model embodies poor predictability for large compounds characterized by a linear scaffold. Nonetheless, the remaining model implies modest to good predictability as summarized in Table 3.

Table 2. Statistical Data for IKKB QSAR Models from Full and Truncated Data Sets Using the Flex-Align Algorithm

IKKB	R^2 training set	Pearson r test set	no. of compounds
clusters with >25 members	0.80	0.78	659
IKKB data set	0.85	0.75	819

Table 3. Correlation Coefficients for Predicted pIC50 Values from the IKKB Flex-Align Model and Experimental pIC50 Values for Clusters with 25 or More Members

cluster no.	no. of compounds	Q^2 [a]	Pearson r
7	53	0.51	0.72
8	37	0.45	0.74
14	53	0.48	0.73
16	202	0.83	0.91
21	128	0.50	0.71
29	65	0.60	0.78
37	82	0.37	0.69
38	40	0.16	0.49

[a]Coefficient of determination for the test set.

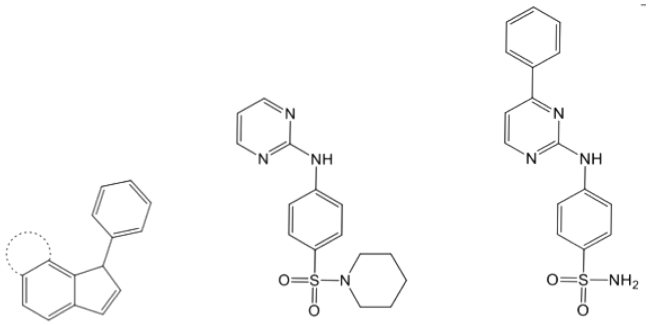

Figure 4. Scaffolds for compound clusters from the IKKB data set.

For IKKA, the four largest clusters, which each have more than 25 members, were also analyzed in parallel with the IKKB data set (Table 4). However, the model obtained from the full IKKA data set is only slightly superior to that of the truncated data set. The four clusters were subsequently predicted by the full IKKA data set model. The largest cluster, cluster 18, provides the best statistical results (Table 5).

Table 4. Statistical Data for IKKA QSAR Models from Full and Truncated Data Sets Using the Flex-Align Algorithm

	training set R^2	test set Pearson r	no. of compounds
IKKA data set	0.83	0.58	384
clusters, >25 members	0.82	0.56	262

It is easy to understand that a larger compound cluster contributes more information to the QSAR model than a smaller one, since the statistical information should be

Table 5. Predicted pIC50 Values and Correlation Coefficients from the IKKA Flex-Align Model for Clusters with More than 25 Members

cluster no.	no. of compounds	Q^2	Pearson r
8	54	0.37	0.71
17	27	0.42	0.72
18	106	0.83	0.92
21	75	0.61	0.79

dx.doi.org/10.1021/ci300287t | J. Chem. Inf. Model. 2012, 52, 3190−3199

Table 6. Statistical Data for 3D-QSAR Models Aligned by Glide Docking

		no. of compounds	R^2	Pearson r	Q^2	training set SD	test set RMSE	no. of outliers
IKKB crystal structure	SP	813	0.71	0.67	0.43	0.60	0.82	41
	XP	819	0.71	0.69	0.46	0.60	0.84	41
IKKB DLG-in model	SP	819	0.78	0.61	0.33	0.52	0.91	45
	XP	819	0.79	0.67	0.40	0.52	0.86	37
IKKA DLG-in model	SP	384	0.85	0.63	0 0.35	0.30	0.62	25
	XP	384	0.77	0.60	0.34	0.37	0.62	16

improved by comparison. The IKKA analysis verifies this assertion. However in the IKKB analysis, the corresponding model delivers poor predictability for cluster 38 with 40 members. Structural analysis for this cluster reveals that all members incorporate a sulfonamide group and present a linear scaffold. Another cluster, cluster 37, shares a scaffold similar to that of cluster 38 and is likewise predicted with low accuracy. We believe there may be other factors behind the poor predictability of IKKB clusters 37 and 38. This point is discussed below in the Type II inhibitor analysis and outliers sections.

Docking Alignment. Glide SP and XP docking studies were also performed on the IKKB data set. Inhibitors were readied with Ligprep[43] and docked into the prepared IKKB crystal structure and the IKKB homology model presenting the DLG-in conformation. The final result retained at most one pose per ligand. For the IKKB homology model, a total of 819 structures were aligned in the ATP binding pocket from the SP and XP dockings. For the IKKB crystal structure, Glide SP docking returned 813 compounds as compared to 819 in the XP docking alignment. For all four IKKB QSAR models, R^2 for the training sets falls near 0.8, while the Pearson r values for the test sets are found from 0.60 to 0.70 (Table 6). In both the Glide SP and XP alignments, the IKKB crystal structure model provides slightly better statistical results than the IKKB homology model. For each protein conformation, the model derived from Glide XP docking alignment reveals higher predictability for the training set than the Glide SP model (Table 6). The best model in the present context was achieved by aligning the IKKB data set in the IKKB crystal structure with Glide XP. The resulting test set Pearson r is 0.69.

In IKKA, both Glide SP and XP furnished 384 aligned compounds. The R^2 and Pearson r values are 0.72 and 0.62 for the SP model and 0.77 and 0.60 for the XP model, respectively. Thus, the Glide SP docking model achieves higher predictability for the test set than the XP model.

Outlier Analysis. Following FB-QSAR model construction, compounds with predicted errors larger than twice the standard division (SD) or twice the root-mean-square of error (RMSE) for test sets were designated as outliers (see Table 6). Both SP and XP models from the IKKB crystal structure yielded 41 outliers (~5%), which can be grouped into five classes on the basis of substitution: nitriles, sulfonamides, four or more monocyclic ring structures tethered by short spacers, compounds with molecular weight less than 300 and the BMS-345541 analogs. Outliers obtained from the IKKB homology model fall into the same classes. Blockers associated with the two IKKA models (25 and 16 from the SP and XP models, respectively, ~5%) segregate into four of the classes mentioned just above, the sulfonamides excepted. In this case, the latter are predicted satisfactorily by the IKKA model. The 18 sulfonamide analogs in this data set provide a superior test set Q^2, 0.64 vs 0.36, and a smaller RMSE, 0.46 vs 0.62, than the average values for the full IKKA data set.

On the basis of the above observations, five compound classes are poorly predicted by FB-QSAR when combined with Glide docking alignment analysis. For the remaining compounds (~95%), the predicted error is within twice the standard deviation. Among the five poorly treated classes, low molecular weight compounds uniformly present a greater number of alternative binding poses than larger systems. Thus, current scoring schemes may not faithfully return correct binding poses for them. For compounds with a nitrile substituent, two of the five outliers fall close to Cys99, an amino acid that carries a nucleophile for potential attack at the nitrile carbon. Were this to be a factor in the in vitro binding event, current docking methodology would not be able to account for such covalent interactions. Sulfonamides present a separate problem, since these analogs frequently coordinate with a metal ion or are surrounded by charged groups in a variety of reported crystal structures. In the active form of the kinases considered here, two metal ions are routinely present for potential chelation by a sulfonamide moiety. However, in our docking studies, such metal ions are absent or neglected, which may lead to an incorrect binding analysis for such compounds. A test of this idea was performed using six protein−sulfonamide complexes from the PDB database, three of which coordinate with metal ions and three of which do not. A typical Glide docking study was performed for each of them. The poses of the latter three complexes without metal ions were well predicted, while none of the metal-complexed forms could be faithfully reproduced (results not shown). Consequently, for inhibitors incorporating sulfonamide or nitrile moieties, poor predictability appears to be the outcome.

A test for the nitrile and sulfonamide compounds in the IKK database was performed to investigate the predictability of the model using the IKKB crystal structure combined with the SP method. With this protocol, the data set derived by removing nitriles or sulfonamides offers a better account of the data (see Table 7, entries 2 and 3). For the considerably truncated set of compounds containing only nitrile or sulfonamide moieties (final entry in Table 7), the model's predictability is at its worst.

Table 7. Examination of Outlier Influence on the Performance of the IKKB Crystal Structure Combined with SP Docking Alignment

	compound no.	Pearson r	Q^2
full data set	813	0.67	0.43
data sets excluding nitrile and sulfonamide compounds	742	0.80	0.64
compounds with only nitriles or sulfonamides	71	0.50	0.24

dx.doi.org/10.1021/ci300287t | J. Chem. Inf. Model. 2012, 52, 3190−3199

(a) BMS-345541 Removal Analysis. One means to determine whether inhibitors are mutually exclusive or not is to perform a multiple inhibition analysis. For IKKB, Burke et al.[4] reported that BMS-345541 binds in a mutually exclusive manner with respect to the peptide mimic IkBa and in a nonmutually exclusive manner with respect to ADP. Contrasting results were obtained for IKKA in which BMS-345541was shown to compete with ADP. These observations imply two possible mechanisms: (1) BMS-345541 binds to the ATP pocket in IKKA but not in IKKB; (2) BMS-345541 binds to the allosteric pocket in both IKKA and IKKB; however, ligand binding alters the peptide binding pocket in IKKB only. The two mechanistic hypotheses agree on an important point: BMS-345541 does not bind to the ATP binding pocket in IKKB. That is to say, regardless of the possible mechanism, neither the flex-align alignment nor the Glide docking placement are suitable for analyzing tricyclic BMS-345541 analogs in the IKKB framework as a result of the ATP noncompetitive binding. Thus, including these compounds in the IKKB data set leads to the increase of noisy information which reduces the predictability of the QSAR model.

The IKKB data set was rechecked to reveal 92 compounds (142 structures after LigPrep treatment) from four literature reports,[22,24,31,37] all of which were generated by modifying BMS-345541. These compounds were gathered in a non-ATP competitor subset of IKKB, while the remaining compounds were assembled in an ATP competitor subset. A preliminary test without the BMS-345541 analogs indicated that SP provides a model in which the training and test set outcomes (R^2 of 0.74 and Pearson r of 0.74, respectively) improve modestly by comparison with the original IKKB model (0.71 and 0.67, respectively). XP docking alignment results in a similar outcome (0.73 and 0.73 vs 0.71 and 0.69, respectively). Thus, removal of BMS-345541 analogs elicits higher predictabilities for both the training and the test sets in the IKKB QSAR model. The result shown in Table 8 is consistent with the idea that BMS-345541 analogs do not bind the ATP binding pocket.

Table 8. Comparison of Statistics for IKKB Data Sets with and without BMS-345541 Analogs

target	docking method	data set	R^2	Pearson r	Q^2
IKKB crystal	SP	IKKB	0.71	0.67	0.43
IKKB crystal	SP	IKKB w/o BMS	0.74	0.74	0.53
IKKB crystal	XP	IKKB	0.71	0.69	0.46
IKKB crystal	XP	IKKB w/o BMS	0.73	0.73	0.52

We also tested the BMS-345541 analogs using the Glide XP alignment and the IKKB DLG-out homology model (R^2 of 0.66 and Pearson r of 0.66), which is somewhat less predictive than the DFG-in model. Three possible factors can account for the diminished accuracy: the DFG-out model is not accurate; BMS-345541 does not bind to the proposed allosteric binding site; or the docking study is unable to predict accurate binding poses as appears to be the case for nitriles and sulfonamides. Using SP scoring, the correlation measures are $R^2 = 0.75$ and Pearson $r = 0.01$. Clearly, FB-QSAR results are highly dependent on the quality of the compound alignment.

(b) Allosteric Type II Kinase Inhibitors. Irina et al.[44] have examined 28 Type II kinase inhibitors complexed with the corresponding kinase targets for which crystal structures have been reported. A comparison of the allosteric Type II kinase inhibitors with known ATP-competing IKK inhibitors (Table 9) indicates that the major physical−chemical properties of the two sets of compounds are significantly different. The molecular weights of type II kinase inhibitors are about 50 Da higher than IKKB inhibitors and about 90 Da higher than IKKA inhibitors, indicating that Type II inhibitors are consistently larger than IKK inhibitors. Volume difference comparisons (Table 9) lead to the same conclusion. On the other hand, the Type II compounds uniformly show low solubility and greater hydrophobicity by comparison. Compounds in the IKKB clusters 37 and 38 derived by flex-align analysis display solubilities and partition coefficients similar to the broad range of IKK inhibitors. However, their molecular weights and volumes are more similar to the Type II inhibitors than the IKK inhibitors. This difference may imply the existence of an allosteric binding pocket similar to that for the Type II blockers. If so, low predictability for the QSAR model focused on ATP binding site substances would be the outcome. It is noteworthy that IKKB outliers with four or more monocyclic rings tethered by a short unbranched linker show higher molecular weights, larger volumes, poorer solubility, and more hydrophobicity than the average IKK inhibitors as illustrated by Table 9. On the basis of the similarity of physical−chemical properties between the four-plus ring-containing outliers and Type II analogs, we speculate that the former compounds are most likely Type II kinase blockers, which target the allosteric binding pocket in IKKB.

Table 9. Physical−Chemical Properties of Type II Kinase Inhibitors, the IKK Inhibitor Data Set, and Selected Subsets

mean	MW(Da)	SASA (Å^2)	PSA (Å^2)	Log S	Log P	volume (Å^3)
type II inhibitors	464	794	87	−6.9	4.7	1407
IKKB inhibitors	415	703	107	−4.7	2.5	1255
IKKA inhibitors	376	651	82	−4.4	2.8	1151
IKKB cluster 37 and 38	444	747	114	−4.6	2.1	1319
selected IKKB outliers	527	828	123	−5.7	3.4	1544

Models from the Truncated Data Sets. As discussed above, the outliers in the five troublesome clusters impart considerable noise to the QSAR models, and thereby limit their predictability. Removal of the corresponding compounds can be expected to improve the quality of the correlation. Accordingly, a series of FB-QSAR models using a variety of truncated data sets were constructed and analyzed as catalogued in Tables 10, 11, and 12. This contingency substantially improves the quality of the QSAR models, especially for the IKKB crystal structure with Glide SP alignment. The Pearson r increases from 0.67 to 0.79, and the corresponding Q^2 (cf. Table 3) for the test set falls above 0.60. Two other truncated data sets were prepared, one by eliminating BMS-345541 analogs and the other by removing compounds with nitrile or sulfonamide moieties. The latter data set yields models with similar quality. However, the best model is provided by Glide XP instead of the SP alignment. For IKKA, a significant upgrade in predictability with the Glide SP alignment was likewise achieved by deletion of outliers. The 18 sulfonamide compounds were excluded and the truncated data set tested separately. The latter furnishes a better statistical result than the full data set model.

Table 10. Comparison of Models from Full and Outlier Delimited Data Sets[a]

		outliers removed				full data sets			
		no. of compounds	R^2	Pearson r	Q^2	no. of compounds	R^2	Pearson r	Q^2
IKKB crystal structure	**SP**	**772**	**0.76**	**0.81**	**0.66**	813	0.71	0.67	0.43
	XP	778	0.81	0.76	0.56	819	0.71	0.69	0.46
IKKB DLG-in model	SP	774	0.76	0.68	0.45	819	0.78	0.61	0.33
	XP	782	0.77	0.72	0.50	819	0.79	0.67	0.40
IKKA DLG-in model	**SP**	**359**	**0.86**	**0.74**	**0.54**	384	0.85	0.63	0 0.35
	XP	368	0.84	0.64	0.40	384	0.77	0.60	0.34

[a]The best models are bolded.

Table 11. Comparison of Full Data Set IKKB Models with Data Sets Devoid of Outliers and BMS-345541 Analogs[a]

		outliers and BMS-345541 analogs removed				full data set			
		no. of compounds	R^2	Pearson r	Q^2	no. of compounds	R^2	Pearson r	Q^2
IKKB crystal structure	SP	619	0.86	0.74	0.52	813	0.71	0.67	0.43
	XP	**624**	**0.83**	**0.78**	**0.59**	819	0.71	0.69	0.46
IKKB DLG-in model	SP	626	0.78	0.71	0.51	819	0.78	0.61	0.33
	XP	636	0.80	0.75	0.56	819	0.79	0.67	0.40

[a]The best model is bolded.

Table 12. Comparison of Full Data Set IKKB Models with Data Sets Devoid of Outliers, BMS-345541 Analogs, Nitriles, and Sulfonamides[a]

		outliers and BMS-345541 analogs nitrile and sulfonamide removed				full data set			
		no. of compounds	R^2	Pearson r	Q^2	no. of compounds	R^2	Pearson r	Q^2
IKKB crystal structure	SP	555	0.90	0.78	0.59	813	0.71	0.67	0.43
	XP	**561**	**0.89**	**0.78**	**0.60**	819	0.71	0.69	0.46
IKKB DLG-in model	SP	563	0.85	0.73	0.50	819	0.78	0.61	0.33
	XP	574	0.85	0.75	0.55	819	0.79	0.67	0.40

[a]The best model is bolded.

Table 13. Comparison of FB-QSAR Model Predictions Resulting from Variation of Random Seeds[a]

data set, protein structure, and docking method	random seed	Q^2	data set, protein structure, and docking method	random seed	Q^2
IKKB crystal XP outlier_BMS nitrile sulfonamide removal	123112	0.60	IKKB model SP outlier_BMS nitrile sulfonamide removal	123112	0.50
	average	0.64		average	0.55
IKKB crystal XP outlier_BMS removal	123112	0.61	IKKB model XP outlier removal	123112	0.50
	average	0.61		average	0.55
IKKb crystal XP outlier removal	123112	0.61	IKKb model XP outlier removal	123112	0.56
	average	0.59		average	0.57
IKKB crystal XP full list	123112	0.46	IKKB crystal SP full list	123112	0.43
	average	0.44		average	0.45
IKKA model XP outlier removal	123112	0.40	IKKA model SP outlier removal	123112	0.54
	average	0.34		average	0.46

[a]The average values of Q^2 correspond to those obtained from using five different seeds: 1000, 5000, 10000, 12345, and 123112.

The truncated data set QSAR models obtained from the IKKB crystal structure consistently yield better predictability than the homology model constructs from P38 MAP kinase. As discussed in the homology modeling section, the crystal structure presents an inactive protein conformer in which its G-rich loop folds into the DLG motif instead of an open conformation as present in the homology model. Due to the high predictability of the crystal structure models, we believe that this inactive conformation of IKKB presents the common binding properties of most of the IKKB Type I inhibitors and, therefore, is the most useful form for rationalizing potency and capturing potential novel IKK inhibitors.

Robustness Evaluations. In the FB-QSAR model generation described above, the training and test sets were assigned a 70−30 split of the data set by using the random split seed 123112 as a constant. In order to investigate the robustness of these FB-QSAR models, alternative models were developed by assigning training and test sets with four arbitrary random split seeds (1000, 5000, 10000, and 12345). The corresponding QSAR models were generated by FB-QSAR. The Q^2 for the corresponding test set is regarded as an index of the predictability of the model. The average value from different models is compared with the model from seed 123112 listed in Table 13. For the IKKB models, the average Q^2 obtained from different random split seeds are similar to that

dx.doi.org/10.1021/ci300287t | J. Chem. Inf. Model. 2012, 52, 3190−3199

Table 14. Predictability Comparison of FB-QSAR and Neural Network Models Obtained from Common Truncated Data Sets

model	data set	compound number	Q^2 (FB-QSAR)	Pearson r (FB-QSAR)	Q^2 (NN)	Pearson r (NN)
IKKB crystal	IKKB data set without outliers	772	0.66	0.81	0.40	0.63
IKKB crystal	IKKB data set without outliers and BMS removal	624	0.59	0.78	10.47	0.69
IKKB crystal	IKKB data set without outliers, BMS, sulfonamide and nitrile removal	561	0.60	0.78	0.56	0.75
IKKA homology model	IKKA data set without outliers	359	0.54	0.74	0.35	0.13

Table 15. Number and Percentage of Active Compounds Retrieved by the QSAR Models

IKKB SP docking outlier removal	compound no.	10	50	100	500	1000	12407
	active compounds no.	10	45	83	118	233	606
	% of active compounds	100	90	83	23.6	23.3	4.88
IKKB XP docking BSM analog and outlier removal	compound no.	10	50	100	500	1000	12407
	active compounds no.	10	42	71	192	257	606
	% of active compounds	100	84	71	38.4	2.57	4.88
IKKA SP docking outlier removal	compound no.	10	50	100	500	1000	12407
	active compounds No.	5	14	18	68	108	299
	% of active compounds	50	28	18	13.6	10.8	2.4

obtained from seed 123112. For IKKA models, the average Q^2 is smaller than that from the same seed. There are two possible reasons for this. The first is the size of the training set, the IKKA magnitude being only half that of the IKKB set. The second is the accuracy of the model. A homology model is generally less accurate than an experimental structure and, thereby, increases the variance of the QSAR model's predictability. The above results indicate that the quality of the FB-QSAR models is relatively insensitive to the way in which the splitting procedure redistributes the data set compounds between the 70% and the 30% components when the size of the training set is large.

In order to investigate the influence of truncated data sets on the QSAR model generation method, models from FB-QSAR and neural network analyses using the same truncated data sets were examined (Table 14). The predictability of neural network models is improved by removing Type II kinase inhibitors but still worse than the FB-QSAR models obtained from the same data sets.

Enrichment Analysis. A decoy data set obtained from the ZINC database was prepared for an enrichment analysis of our best models. This 10 000 compound data set was constructed to exclude IKK inhibitors and to incorporate diverse molecular weights (MW 200−500). It was then merged with 224 and 500 IKKA and IKKB inhibitors, respectively, the binding affinities of which are less than 10 μM. Two IKKB and one IKKA models (Table 15) were applied to the decoy database to predict active inhibitors. Structures in the top 50 hits with the highest predicted IC_{50} values were examined to ascertain if they are true IKK inhibitors. Over 70% of the top hits appear in the IKKB inhibitor data set with binding affinities <10 μM. This is over 14 times higher than the enrichment of the whole database. For IKKA, due to the lack of a crystal structure, the QSAR model obtained from our homology model is expected to provide reduced accuracy relative to an experimental structure. However, the hit rate for the top 50 compounds using the IKKA model is still 10 times higher than the enrichment of the whole database. This indicates that, even with a homology model-based QSAR, our protocol still can retrieve active compounds with a high hit rate. These outcomes seem to confirm what appears to be an outstanding predictability of our QSAR models for virtual screening.

CONCLUSIONS

In this study, homology models for the IKKA and IKKB proteins were constructed in order to analyze IKK inhibitor binding properties. In most reported structure-based kinase inhibitor searches, type I kinase inhibitors have been assumed to compete with ATP, which binds to the active form of the kinase. Compared with the current homology models obtained from the active form of P38 MAP kinase, the recently reported IKKB crystal structure adopts an inactive conformation induced upon inhibitor binding, which is not similar to the active form of typical kinases. A comparison of the two protein conformations as they pertain to inhibitor binding was performed to explore which form might correspond to the actual inhibitor bound form of IKKB. Utilizing the IKKB crystal structure, IKK homology models, and the IKK inhibitor data found in the Binding Database, a series of QSAR models was generated employing different methods. Models constructed by the FB-QSAR approach combined with a truncated database prepared by Glide SP alignment provide the best predictability for the current data set. The truncated database was generated by removing five classes of outliers from the full IKK inhibitor data set, thereby shrinking the combined IKKA and IKKB inhibitor database by 5%. The outlier analysis demonstrates that the five classes cannot be accurately predicted by any of the models explored. It is suggested that BMS-345541 analogs and large MW compounds with four or more monocyclic rings tethered by short linkages are possibly Type II kinase inhibitors which appear to bind to an allosteric binding pocket separate from that occupied by ATP. Small compounds with a molecular weight below 300 and analogs carrying a nitrile or sulfonamide moiety are also poorly predicted with the current models. We speculate this may be due to inaccurate pose predictions by Glide. By removing these outliers, the models' predictive accuracy is significantly improved from 41% to 61% (reflected by Q^2 for the test set) for IKKB and from 35% to 54% for IKKA. The corresponding R^2 values for the training sets are also improved slightly from 0.71 to 0.78 for IKKB and 0.85 to 0.86 for IKKA. Accordingly, the models using truncated data

sets deliver better predictabilities for both the training sets and the corresponding test sets and provide an efficient method for extracting novel IKK inhibitor candidates from commercial or in-house databases. Due to the poor predictability for the five outlier classes, candidate inhibitor databases should be prepared without such compounds when utilizing the current QSAR models.

Compared with the IKKB crystal structure and the IKKA homology model, each presenting the DLG-in conformation, QSAR expressions obtained from the IKKB DLG-in and DLG-out homology models gave moderately lower predictability. This is most likely the result of the low sequence identity between IKKB and the P38 MAP kinase crystal template, 33% for IKKB and the DFG-in P38 MAP kinase. The corresponding comparison for DFG-out P38 MAP kinase is only 18%. The latter is at the edge of the 20% residue identity boundary for acceptable homology model generation. Clearly, considerable noise is sustained by the QSARs based on these less precise homology structures. Consequently, predictability is reduced for test sets as reflected by a lower Pearson r and Q^2.

The present analysis also suggests that QSAR models refined with an inactive form of IKKB, characterized by a closed conformation of the G-rich loop, deliver higher predictability than those derived from an open and active conformation. This observation implies that IKKB may prefer the inactive form in the crystalline state when complexed with an inhibitor as recently observed[45] and perhaps in any future IKKB-ligand complexes as well. Namely, competitive inhibitor binding may trigger two reinforcing processes. The first clearly involves displacement of ATP to eliminate the phosphorylating agent, while the second step may induce the kinase to adopt a closed conformation hindering ligand off-rate. While the observation that the superior QSAR model described above operates through the inactive conformation is not sufficient to prove this assertion, it is certainly consistent with it. This hypothesis differs from the general assumption that an ATP competitive kinase inhibitor should bind to the same binding pocket conformation as ATP. It will be of interest to learn if this observation is general for the entire range of known kinase families.

EXPERIMENTAL SECTION

Homology Model Generation. Sequences of IKKA and IKKB proteins were obtained from the National Center for Biotechnology Information (NCBI). Protein crystal structures similar to IKKB were retrieved using Blast embedded in Prime3.1. The crystal structure with the highest identity, P38 MAP kinase (33%, PDB ID 1CM8), was selected as a template for IKKB with the DLG-in conformation. Due to the lack of the G-rich loop in 1CM8, another kinase, ribosomal protein S6 kinase (PDB ID 2Z7R) which shares high similarity in the G-rich loop region with IKKB, was selected to supplement the missing G-rich loop in 1CM8. The ligand AMP-PNP in 1CM8 was preserved when generating the IKKB homology model with Modeler v9.1 and refined by Prime3.1. The IKKA active homology model was generated with the same protocol by using the IKKB crystal structure as template (PDB ID 3RZF). The two IKK subunits share 58% sequence identity and 69% similarity. The resulting IKKA and IKKB models were then evaluated with ProcheckV3.0 and rerefined by Prime iteratively until the G-factor was either above −0.50 (IKKB DLG-in and out) or similar to the corresponding template (IKKA DLG-in).

As part of the generation of the IKKB DLG-out homology model, ClustalW[46] was utilized to align the sequence of IKKB with 28 kinases in which crystal structures with the DFG-out conformation were reported. Such DFG-out conformations are believed to be induced during Type II kinase inhibitor binding. The structure with the highest sequence identity, an inactive form of P38 MAP kinase (PDB ID 1WBN; 17% identity and 28% similarity) was selected as template. The initial inactive form of the IKKB DLG-out homology model was constructed with Modeler v9.1; the rough model being refined by Prime3.1 and checked by ProCheckV3.0[47] (see Table 16).

Table 16. ProCheck G-factor Measurements[a]

	dihedral angles[b](deg)	main-chain covalent force[c]	overall average[d]
1CM8	0.10	0.47	0.25
IKKB DLG-in	−0.28	−0.29	−0.27
1WBN	−0.17	0.62	0.14
IKKB DLG-out	−0.25	−0.29	−0.26
3RZF	−0.71	−0.30	−0.52
IKKA DLG-in	−0.46	−0.57	−0.52

[a]All structural data are compared with the Enghand-Huber (1991) ideal values derived from small-molecule data. [b]The dihedral angles include Phi−Psi, Chi1−Chi2, Chi1 only, Chi3, Chi4, and the Omega distribution. [c]Main-chain covalent forces contain main-chain bond lengths and main-chain bond angles. [d]The overall average includes both the dihedral angles and the main-chain covalent forces.

Database of IKK Inhibitors. An extensive collection of IKK inhibitors was obtained from The Binding Database, a public, web-accessible database of measured binding affinities. The database contains two subsets: an IKKA subset with 358 compounds and an IKKB subset with 768 compounds. Since most of the reported binding affinities are characterized by an "Enzymologic IC_{50}", those compounds without this designation were excluded to provide a filtered database with 285 and 662 compounds for IKKA and IKKB, respectively. Tautomer and ionization predictions were performed on IKK data set members with LigPrep2.5. Finally, 384 and 819 structures for the IKKA and IKKB subsets, respectively, were obtained to generate a refined IKK inhibitor database. The database and the FB-QSAR models are available via the Supporting Information.

Neural Network Analysis. Neural network analysis was performed with Canvas 1.5 utilizing energy descriptors obtained from Glide SP, Glide XP, or Glide SP with Prime MMGBSA rescoring. 70% of the compounds in the IKK databases were assigned to the training set accompanied by a selected random selected seed. The total number of networks trained was 20; the best 5 of which were retained. The number of training cycles was the default value, 200.

Flex-Align. Flex-align is one of the utilities embedded in the Schrodinger Suite2011. It utilizes the Phase Shape method to align the compounds of a given database with a user-defined template or a compound in the database presenting the shortest distance from the rest of the compounds in the same database. Structures of compounds in the IKKB data set were clustered with the hierarchical clustering dendrogram in Canvas1.5 using the Kelley criterion. The entire data set as well structures in different clusters were aligned by Flex-align for the FB-QSAR model generation.

Field-Based QSAR. Field-based QSAR was performed by the application incorporated in the Schrodinger Suite 2011.

IC_{50} values for the compounds in the data set were obtained from BindingDB. In the FB-QSAR model generation step, 70% of the compounds were randomly selected as training set and the random seed was set as 123112. The model generation was based on Gaussian type force field, and the maximum PLS factors number were set to 10. Default values were accepted for all other options. The best model is characterized by the highest Q^2 and Pearson r and R^2 values between 0.6 and 0.9.

Enrichment Analysis. For this, 10 000 compounds were selected from the ZINC database with the same distribution of molecular weights as the entire database and labeled as IKK inactive. The separate subdata sets of IKKA and IKKB from ZINC were labeled as IKKA or IKKB inhibitors and merged with the prepared IKK inactive data set. The merged data set was prepared with LigPrep and docked into our IKK models with Glide 5.8. Binding affinities for all compounds in the merged collection were subsequently predicted by the best IKKA and IKKB models.

■ ASSOCIATED CONTENT

Ⓢ Supporting Information

Data sets for IKK inhibitors, docking Grid files, field-based QSAR models, and the enrichment data set. This material is available free of charge via the Internet at http://pubs.acs.org.

■ AUTHOR INFORMATION

Corresponding Author

*E-mail: hhu2@emory.edu (H.H.); jsnyder@emory.edu (J.P.S.).

Notes

The authors declare no competing financial interest.

■ ACKNOWLEDGMENTS

We are grateful to Prof. Dennis Liotta (Emory University) for generous support and to Dr. Pahk Thepchatri and Dr. Andy Prussia (EIDD, Emory University) for numerous insightful discussions.

■ REFERENCES

(1) Strnad, J.; Burke, J. R. IkappaB kinase inhibitors for treating autoimmune and inflammatory disorders: potential and challenges. *Trends Pharmacol. Sci.* **2007**, *28*, 142−148.

(2) Zandi, E.; Rothwarf, D. M.; Delhase, M.; Hayakawa, M.; Karin, M. The IKB Kinase Complex (IKK) Contains Two Kinase Subunits, IKKA and IKKB, Necessary for IK B Phosphorylation and NF- KB Activation. *Cell* **1997**, *91*, 243−252.

(3) Ghosh, S.; Karin, M.; Haven, N. Missing Pieces in the NF-κB Puzzle. *Cell* **2002**, *109*, S81−96.

(4) Burke, J. R.; Pattoli, M. a; Gregor, K. R.; Brassil, P. J.; MacMaster, J. F.; McIntyre, K. W.; Yang, X.; Iotzova, V. S.; Clarke, W.; Strnad, J.; Qiu, Y.; Zusi, F. C. BMS-345541 is a highly selective inhibitor of I kappa B kinase that binds at an allosteric site of the enzyme and blocks NF-kappa B-dependent transcription in mice. *J. Biol. Chem.* **2003**, *278*, 1450−1456.

(5) Ziegelbauer, K.; Gantner, F.; Lukacs, N. W.; Berlin, A.; Fuchikami, K.; Niki, T.; Sakai, K.; Inbe, H.; Takeshita, K.; Ishimori, M.; Komura, H.; Murata, T.; Lowinger, T.; Bacon, K. B. A selective novel low-molecular-weight inhibitor of IkappaB kinase-beta (IKK-beta) prevents pulmonary inflammation and shows broad anti-inflammatory activity. *Br. J. Pharmacol.* **2005**, *145*, 178−192.

(6) Liu, T.; Lin, Y.; Wen, X.; Jorissen, R. N.; Gilson, M. K. BindingDB: a web-accessible database of experimentally determined protein-ligand binding affinities. *Nucleic Acids Res.* **2007**, *35*, D198−201.

(7) Eswar, N.; Eramian, D.; Webb, B.; Shen, M.-yi; Sali, A. Protein structure modeling with MODELLER. *Methods Mol. Biol.* **2008**, *426*, 145−59.

(8) *Prime*, version 3.1; Schrödinger, LLC, New York, 2012.

(9) *Glide*, version 5.8; Schrödinger, LLC, New York, 2012.

(10) Hopfield, J. J. Neural networks and physical systems with emergent collective computational abilities. *Proc. Nat. Acad. Sci.* **1982**, *79*, 2554−2558.

(11) *Canvas*, version 1.4; Schrödinger, LLC, New York, 2011.

(12) *Phase*, version 3.3; Schrödinger, LLC, New York, 2011.

(13) FB-QSAR utilizes Gaussian functions to fit the interactions described. The general form of the force field is

$$F_X = \sum_j X_j \exp(-\alpha r_{ij}^2)$$

(14) Tetko, I. V.; Livingstone, D. J.; Luik, A. I. Neural network studies. 1. Comparison of overfitting and overtraining. *J. Chem. Inf. Comput. Sci.* **1995**, *35*, 826−833.

(15) Castro, A. C.; Dang, L. C.; Soucy, F.; Grenier, L.; Mazdiyasni, H.; Hottelet, M.; Parent, L.; Pien, C.; Palombella, V.; Adams, J.; Novel, I. K. K. inhibitors: β-carbolines. *Bioorg. Med. Chem. Lett.* **2003**, *13*, 2419−2422.

(16) Bingham, A. H.; Davenport, R. J.; Gowers, L.; Knight, R. L.; Lowe, C.; Owen, D. a.; Parry, D. M.; Pitt, W. R. A novel series of potent and selective IKK2 inhibitors. *Bioorg. Med. Chem. Lett.* **2004**, *14*, 409−412.

(17) Murata, T.; Shimada, M.; Kadono, H.; Sakakibara, S.; Yoshino, T.; Masuda, T.; Shimazaki, M.; Shintani, T.; Fuchikami, K.; Bacon, K. B.; Ziegelbauer, K. B.; Lowinger, T. B. Synthesis and structure-activity relationships of novel IKK-beta inhibitors. Part 2: Improvement of in vitro activity. *Bioorg. Med. Chem. Lett.* **2004**, *14*, 4013−4017.

(18) Murata, T.; Shimada, M.; Sakakibara, S.; Yoshino, T.; Masuda, T.; Shintani, T.; Sato, H.; Koriyama, Y.; Fukushima, K.; Nunami, N.; Yamauchi, M.; Fuchikami, K.; Komura, H.; Watanabe, A.; Ziegelbauer, K. B.; Bacon, K. B.; Lowinger, T. B. Synthesis and structure-activity relationships of novel IKK-beta inhibitors. Part 3: Orally active anti-inflammatory agents. *Bioorg. Med. Chem. Lett.* **2004**, *14*, 4019−4022.

(19) Bonafoux, D.; Bonar, S.; Christine, L.; Clare, M.; Donnelly, A.; Guzova, J.; Kishore, N.; Lennon, P.; Libby, A.; Mathialagan, S.; McGhee, W.; Rouw, S.; Sommers, C.; Tollefson, M.; Tripp, C.; Weier, R.; Wolfson, S.; Min, Y. Inhibition of IKK-2 by 2-[(aminocarbonyl)-amino]-5-acetylenyl-3-thiophenecarbox-amides. *Bioorg. Med. Chem. Lett.* **2005**, *14*, 2870−2875.

(20) Waelchli, R.; Bollbuck, B.; Bruns, C.; Buhl, T.; Eder, J.; Feifel, R.; Hersperger, R.; Janser, P.; Revesz, L.; Zerwes, H. G.; Schlapbach, A. Design and preparation of 2-benzamido-pyrimidines as inhibitors of IKK. *Bioorg. Med. Chem. Lett.* **2006**, *16*, 108−112.

(21) Morwick, T.; Berry, A.; Brickwood, J.; Cardozo, M.; Catron, K.; DeTuri, M.; Emeigh, J.; Homon, C.; Hrapchak, M.; Jacober, S.; Kaplita, P.; Kelly, T. A.; Ksiazek, J.; Liuzzi, M.; Magolda, R.; Mao, C.; Marshall, D.; McNeil, D.; Prokopowicz, A., 3rd; Sarko, C.; Scouten, E.; Sledziona, C.; Sun, S.; Watrous, J.; Wu, J. P.; Cywin, C. L Evolution of the thienopyridine class of inhibitors of IkappaB kinase-beta: part I: hit-to-lead strategies. *J. Med. Chem.* **2006**, *49*, 2898−2908.

(22) Bain, J.; Plater, L.; Elliott, M.; Shpiro, N.; Hastie, C. J.; McLauchlan, H.; Klevernic, I.; Arthur, J. S. C.; Alessi, D. R.; Cohen, P. The selectivity of protein kinase inhibitors: a further update. *Biophys. J.* **2007**, *408*, 297−315.

(23) Beaulieu, F.; Ouellet, C.; Ruediger, E. H.; Belema, M.; Qiu, Y.; Yang, X.; Banville, J.; Burke, J. R.; Gregor, K. R.; MacMaster, J. F.; Martel, A.; Mclntyre, K. W.; Pattoli, M. A.; Zusi, F. C.; Vyas, D. Synthesis and biological evaluation of 4-amino derivatives of benzimidazoquinoxaline, benzimidazoquinoline, and benzopyrazolo-quinazoline as potent IKK inhibitors. *Bioorg. Med. Chem. Lett.* **2007**, *17*, 1233−1237.

(24) Christopher, J. a; Avitabile, B. G.; Bamborough, P.; Champigny, A. C.; Cutler, G. J.; Dyos, S. L.; Grace, K. G.; Kerns, J. K.; Kitson, J. D.; Mellor, G. W.; Morey, J. V.; Morse, M. A.; O'Malley, C. F.; Patel, C. B.; Probst, N.; Rumsey, W.; Smith, C. A.; Wilson, M. J. The discovery

of 2-amino-3,5-diarylbenzamide inhibitors of IKK-alpha and IKK-beta kinases. *Bioorg. Med. Chem. Lett.* **2007**, *17*, 3972−3977.
(25) Belema, M.; Bunker, A.; Nguyen, V. N.; Beaulieu, F.; Ouellet, C.; Qiu, Y.; Zhang, Y.; Martel, A.; Burke, J. R.; Mclntyre, K. W.; Pattoli, M. A.; Daloisio, C.; Gillooly, K. M.; Clarke, W. J.; Brassil, P. J.; Zusi, F. C.; Vyas, D. M. Synthesis and structure-activity relationship of imidazo(1,2-a)thieno(3,2-e) pyrazines as IKK-beta inhibitors. *Bioorg. Med. Chem. Lett.* **2007**, *17*, 4284−4289.
(26) Bamborough, P.; Drewry, D.; Harper, G.; Smith, G. K.; Schneider, K. Assessment of chemical coverage of kinome space and its implications for kinase drug discovery. *J. Med. Chem.* **2008**, *51*, 7898−7914.
(27) Christopher, J. a; Bamborough, P.; Alder, C.; Campbell, A.; Cutler, G. J.; Down, K.; Hamadi, A. M.; Jolly, A. M.; Kerns, J. K.; Lucas, F. S.; Mellor, G. W.; Miller, D. D.; Morse, M. A.; Pancholi, K. D.; Rumsey, W.; Solanke, Y. E.; Williamson, R. Discovery of 6-aryl-7-alkoxyisoquinoline inhibitors of IkappaB kinase-beta (IKK-beta). *J. Med. Chem.* **2009**, *52*, 3098−3102.
(28) Kempson, J.; Guo, J.; Das, J.; Moquin, R. V.; Spergel, S. H.; Watterson, S. H.; Langevine, C. M.; Dyckman, A. J.; Pattoli, M.; Burke, J. R.; Yang, X. X.; Gillooly, K. M.; Mclntyre, K. W.; Chen, L.; Dodd, J. H.; McKinnon, M.; Barrish, J. C.; Pitts, W. J. Synthesis, initial SAR and biological evaluation of 1,6-dihydroimidazo[4,5-d]pyrrolo[2,3-b]-pyridin-4-amine derived inhibitors of IkappaB kinase. *Bioorg. Med. Chem. Lett.* **2009**, *19*, 2646−2649.
(29) Nagarajan, S.; Doddareddy, M. R.; Choo, H.; Cho, Y. S.; Oh, K.-S.; Lee, B. H.; Pae, A. N. IKKbeta inhibitors identification part I: homology model assisted structure based virtual screening. *Bioorg. Med. Chem.* **2009**, *17*, 2759−2766.
(30) Nagarajan, S.; Doddareddy, M. R.; Choo, H.; Cho, Y. S.; Oh, K.-S.; Lee, B. H.; Pae, A. N. IKKbeta inhibitors identification part I: homology model assisted structure based virtual screening. *Bioorg. Med. Chem.* **2009**, *17*, 2759−2766.
(31) Nagarajan, S.; Choo, H.; Cho, Y. S.; Oh, K.-S.; Lee, B. H.; Shin, K. J.; Pae, A. N. IKKbeta inhibitors identification part II: ligand and structure-based virtual screening. *Bioorg. Med. Chem.* **2010**, *18*, 3951−3960.
(32) Bonafoux, D. F.; Bonar, S. L.; Clare, M.; Donnelly, A. M.; Glaenzer, J. L.; Guzova, J. a; Huang, H.; Kishore, N.N.; Koszyk, F J.; Lennon, P. J.; Libby, A.; Mathialagan, S.; Oburn, D. S.; Rouw, S. A.; Sommers, C. D.; Tripp, C. S.; Vanella, L. J.; Weier, R.; Wolfson, S. G.; Huang, H. C. Aminopyridinecarboxamide-based inhibitors: Structure-activity relationship. *Bioorg. Med. Chem.* **2010**, *18*, 403−414.
(33) Bhattarai, B. R.; Ko, J.-H.; Shrestha, S.; Kafle, B.; Cho, H.; Kang, J.-H.; Cho, H. Inhibition of IKK-beta: a new development in the mechanism of the anti-obesity effects of PTP1B inhibitors SA18 and SA32. *Bioorg. Med. Chem. Lett.* **2010**, *20*, 1075−1077.
(34) Crombie, A. L.; Sum, F.-W.; Powell, D. W.; Hopper, D. W.; Torres, N.; Berger, D. M.; Zhang, Y.; Cavriil, M.; Sadler, T. M.; Arndt, K. Synthesis and biological evaluation of tricyclic anilinopyrimidines as IKKbeta inhibitors. *Bioorg. Med. Chem. Lett.* **2010**, *20*, 3821−3825.
(35) Shimizu, H.; Tanaka, S.; Toki, T.; Yasumatsu, I.; Akimoto, T.; Morishita, K.; Yamasaki, T.; Yasukochi, T.; Iimura, S. Discovery of imidazo[1,2-b]pyridazine derivatives as IKKbeta inhibitors. Part 1: Hit-to-lead study and structure-activity relationship. *Bioorg. Med. Chem. Lett.* **2010**, *20*, 5113−5118.
(36) Noha, S. M.; Atanasov, A. G.; Schuster, D.; Markt, P.; Fakhrudin, N.; Heiss, E. H.; Schrammel, O.; Rollinger, J. M.; Stuppner, H.; Dirsch, V. M.; Wolber, G. Discovery of a novel IKK-β inhibitor by ligand-based virtual screening techniques. *Bioorg. Med. Chem. Lett.* **2011**, *21*, 577−583.
(37) Xie, J.; Poda, G. I.; Hu, Y.; Chen, N. X.; Heier, R. F.; Wolfson, S. G.; Reding, M. T.; Lennon, P. J.; Kurumbail, R. G.; Selness, S. R.; Li, X.; Kishore, N. N; Sommers, C. D.; Christine, L.; Bonar, S. L.; Venkatraman, N.; Mathialagan, S.; Brustkern, S. J.; Huang, H. C. Aminopyridinecarboxamide-based inhaled IKK-2 inhibitors for asthma and COPD: Structure-activity relationship. *Bioorg. Med. Chem.* **2011**, *19*, 1242−1255.
(38) Dyckman, A. J.; Langevine, C. M.; Quesnelle, C.; Kempson, J.; Guo, J.; Gill, P.; Spergel, S. H.; Watterson, S. H.; Li, T.; Nirschl, D. S.; Gillooly, K. M.; Pattoli, M. A.; Mclntyre, K. W.; Chen, L.; McKinnon, M.; Dood, J. H.; Barrish, J. C.; Burke, J. R.; Pitts, W. J. Imidazo[4,5-d]thiazolo[5,4-b]pyridine based inhibitors of IKK2: synthesis, SAR, PK/PD and activity in a preclinical model of rheumatoid arthritis. *Bioorg. Med. Chem. Lett.* **2011**, *21*, 383−386.
(39) Shimizu, H.; Yasumatsu, I.; Hamada, T.; Yoneda, Y.; Yamasaki, T.; Tanaka, S.; Toki, T.; Yokoyama, M.; Morishita, K.; Iimura, S. Discovery of imidazo[1,2-b]pyridazines as IKKβ inhibitors. Part 2: improvement of potency in vitro and in vivo. *Bioorg. Med. Chem. Lett.* **2011**, *21*, 904−908.
(40) Takahashi, H.; Shinoyama, M.; Komine, T.; Nagao, M.; Suzuki, M.; Tsuchida, H.; Katsuyama, K. Novel dihydrothieno[2,3-*e*]indazole derivatives as IκB kinase inhibitors. *Bioorg. Med. Chem. Lett.* **2011**, *21*, 1758−1762.
(41) Avila, C. M.; Lopes, A. B.; Gonçalves, A. S.; da Silva, L. L.; Romeiro, N. C.; Miranda, A. L. P.; Sant'Anna, C. M. R.; Barreiro, E. J.; Fraga, C. a M. Structure-based design and biological profile of (*E*)-*N*-(4-Nitrobenzylidene)-2-naphthohydrazide, a novel small molecule inhibitor of IκB kinase-β. *Eur. J. Med. Chem.* **2011**, *46*, 1245−1253.
(42) Kempson, J.; Spergel, S. H.; Guo, J.; Quesnelle, C.; Gill, P.; Belanger, D.; Dyckman, A. J.; Li, T.; Watterson, S. H.; Langevine, C. M.; Das, J.; Moquin, R. V.; Furch, J. A.; Marinier, A.; Dodier, M.; Martel, A.; Nirschl, D.; VanKirk, K.; Burke, J. R.; Pattoli, M. A.; Gillooly, K.; McIntyre, K. W.; Chen, L.; Yang, Z.; Marathe, P. H.; Wang-Iverson, D.; Dodd, J. H.; McKinnon, M.; Barrish, J. C.; Pitts, W. J. Novel tricyclic inhibitors of IkappaB kinase. *J. Med. Chem.* **2009**, *52*, 1994−2005.
(43) *LigPrep*, version 2.5; Schrödinger, LLC, New York, 2011.
(44) Irina, K.; Ruben, A. Type-II kinase inhibitor docking, screening, and profiling using modified structures of active kinase states. *J. Med. Chem.* **2008**, *51*, 7921−7932.
(45) Xu, G.; Lo, Y. C.; Li, Q.; Napolitano, G.; Wu, X.; Jiang, X.; Dreano, M.; Karin, M.; Wu, H. Crystal structure of inhibitor of κB kinase β (IKKβ). *Nature* **2011**, *21*, 325−330.
(46) Larkin, M. a; Blackshields, G.; Brown, N. P.; Chenna, R.; McGettigan, P. a; McWilliam, H.; Valentin, F.; Wallace, I. M.; Wilm, a; Lopez, R.; Thompson, J. D.; Gibson, T. J.; Higgins, D. G. Clustal W. and Clustal X. version 2.0. *Bioinformatics* **2007**, *23*, 2947−2948.
(47) Laskowski, R. A.; MacArthur, M. W.; Moss, D. S.; Thornton, J. M. *PROCHECK*: a program to check the stereo chemical quality of protein structures. *J. Appl. Crystallogr.* **1993**, *26*, 283−291.